Letter

Unraveling the origin of the peculiar transition in the magnetically ordered phase of the Weyl semimetal $Co_3Sn_2S_2$

Ivica Živković,[1,*] Ravi Yadav,[2] Jian-Rui Soh,[1] ChangJiang Yi,[3,4] YouGuo Shi,[4,5,6] Oleg V. Yazyev,[2] and Henrik M. Rønnow[1]

[1]*Laboratory for Quantum Magnetism, Institute of Physics, École Polytechnique Fédérale de Lausanne, CH-1015 Lausanne, Switzerland*
[2]*Institute of Physics, École Polytechnique Fédérale de Lausanne, CH-1015 Lausanne, Switzerland*
[3]*Department of Solid State Chemistry, Max Planck Institute for Chemical Physics of Solids, D-01187 Dresden, Germany*
[4]*Beijing National Laboratory for Condensed Matter Physics, Institute of Physics, Chinese Academy of Sciences, Beijing 100190, China*
[5]*School of Physical Sciences, University of Chinese Academy of Sciences, Beijing 100190, China*
[6]*Songshan Lake Materials Laboratory, Dongguan 523808, China*

(Received 6 April 2022; revised 27 September 2022; accepted 1 November 2022; published 21 November 2022)

The recent discovery of topologically nontrivial behavior in $Co_3Sn_2S_2$ stimulated a notable interest in this itinerant ferromagnet ($T_C = 174$ K). The exact magnetic state remains ambiguous, with several reports indicating the existence of a second transition in the range 125–130 K, with antiferromagnetic and glassy phases proposed to coexist with the ferromagnetic phase. Using detailed angle-dependent dc and ac magnetization measurements on large, high-quality single crystals we reveal a highly anisotropic behavior of both the static and dynamic response of $Co_3Sn_2S_2$. It is established that many observations related to sharp magnetization changes when $B \parallel c$ are influenced by the demagnetization factor of a sample. On the other hand, a genuine transition has been found at $T_P = 128$ K, with the magnetic response being strictly perpendicular to the c axis and several orders of magnitude smaller than for $B \parallel c$. Calculations using density-functional theory indicate that the ground state magnetic structure consist of magnetic moments canted away from the c axis by a small angle ($\sim 1.5^\circ$). We argue that the second transition originates from a small additional canting of moments within the kagome plane, with two equivalent orientations for each spin.

DOI: 10.1103/PhysRevB.106.L180403

Topology and topological properties of matter have recently gained a lot of attention due to the realization of their importance in various exotic phases such as topological insulators [1], Dirac and Weyl (semi)metals [2], and spin liquids [3]. The band structure of topologically nontrivial compounds is strongly influenced by spin-orbit coupling (SOC), leading to band inversion and relativistic fermions with linear dispersions. Depending on whether the spatial ($\mathcal{P}$) and time-reversal ($\mathcal{T}$) symmetries are preserved or broken, the crossing points of such inverted bands are called Dirac or Weyl nodes, respectively. If Weyl nodes are found close to the Fermi energy they can strongly affect the transport properties due to the fact that the nodes act as sources of Berry curvature [4]. The control of topological properties using external parameters is highly sought after, offering a novel type of topological phase transitions. In systems with broken $\mathcal{P}$ this is hard to realize, as they are intrinsically linked to the underlying crystal structure. On the other hand, $\mathcal{T}$ breaking is related to the appearance of magnetic order, allowing temperature T or magnetic field B to tune topological invariants and drive the system across a topological phase transition.

It has been recently suggested that $Co_3Sn_2S_2$ is a Weyl semimetal [5,6], exhibiting ferromagnetic (FM) order below $T_C = 174$ K [7]. Evidence of topologically nontrivial behavior includes the anomalous Hall effect [5], the visualization of surface Fermi arcs [6,8], and the giant magneto-optical response [9]. These are considered to arise from the existence of Weyl nodes with opposite chirality [2], whose number and position relative to the Fermi energy are strongly influenced by the details of the magnetic order. It has been established that the value of the magnetic moment on Co ions is directly linked to the separation of Weyl nodes in the k space [10] while controlling the direction of magnetization allows to shift, create, and annihilate Weyl nodes [11].

The FM order is associated with itinerant electrons originating from d orbitals of Co ions ($\sim 0.3\mu_B$/Co), arranged in kagome layers [sketched in Fig. 1(a)] and stacked along the c axis in the A-B-C pattern [7]. Such a reduced value of the magnetic moment has recently been explained within the local triangular Co cluster, giving rise to a $S = 1/2$ state ($=1\mu_B$) over three Co ions. It has been indicated numerically [12] and experimentally [13] that the moment is aligned parallel to the c axis, with a field of 23 T needed to fully orient the moment parallel to the kagome plane [13].

This simple configuration has been recently challenged by a muon-spin rotation (μSR) study, indicating that just below T_C the FM order is accompanied by a second phase, interpreted as an antiferromagnetic (AFM) arrangement of in-plane moments forming a type of a 120° configuration [14]. The second phase appears above 90 K, reaching almost 70% of the volume fraction just below T_C. Those conclusions

*ivica.zivkovic@epfl.ch

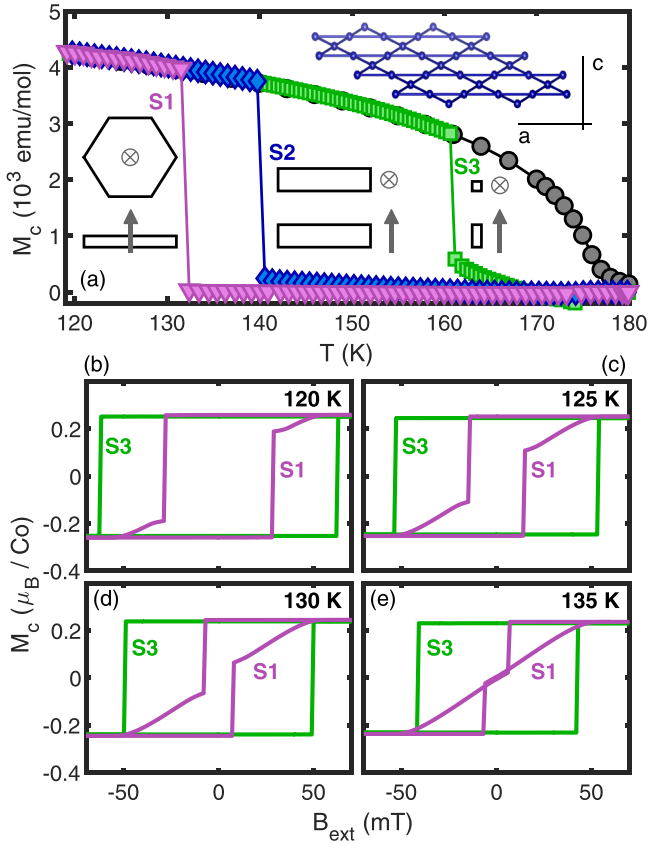

FIG. 1. (a) $M \parallel c$ vs temperature for samples $S1$, $S2$, and $S3$ following the FC/ZFW protocol. The samples were cooled down in $B_{\text{ext}} = 10$ mT (black circles). The arrows and crosses indicate the direction of the c axis. The panel also shows a single kagome plane of Co atoms. (b)–(e) Hysteresis curves for samples $S1$ and $S3$.

have been called into question by a recent polarized neutron study [15], severely limiting the extent of a *coherent* AFM phase. Additionally, a second transition has been suggested to appear in the range 125–130 K based on dc and ac magnetization measurements [16]. Further experimental evidence for its presence has been accumulated by resistivity and magnetization [17], magneto-optical Kerr effect studies [18], and neutron diffraction [15], although the exact temperature of the transition has been shown to differ from one study to the other. The observation of shifted, magnetic-field-driven hysteresis at low temperatures has been ascribed to an exchange bias mechanism and associated with the appearance of a glassy state below 125 K [17].

In this Letter, we aim to clarify several confusing, and often contradicting findings related to the magnetic order in $Co_3Sn_2S_2$. We clearly establish a strongly direction-dependent magnetic response and reveal that for $B \parallel c$ it is largely dominated by the demagnetization factor. For $B \perp c$ a second transition is found at $T_P = 128$ K, with the magnetic component strictly confined to the kagome plane, indicating a small canting of magnetic moments on Co ions. We confirm the canting scenario by performing careful density-functional theory (DFT) calculations, revealing the umbrella structure where moments on a triangle tilt towards its center.

High-quality single crystals were grown by the self-flux method and characterized in previous publications [6,15,19]. The dc and ac magnetizations were measured on a superconducting quantum interference device (SQUID)-based magnetometer (MPMS3, Quantum Design) equipped with a horizontal rotator, allowing an angular precision better than 0.1°. Three samples have been used throughout this study, cut from the same large single crystal, and their dimensions and masses are detailed in the Supplemental Material [20]. DFT calculations were performed using the Vienna *ab initio* simulation package (VASP) [21,22] on periodic models of the experimental crystal structure [23]. Electron-core interactions were described with the projector augmented-wave method, while the Kohn-Sham wave functions for the valence electrons were expanded in a plane-wave basis with a cutoff of 500 eV on the kinetic energy. We used a mesh of $11\times11\times11$ k points and the Perdew-Burke-Ernzerhof (PBE) variant [24] of the generalized gradient approximation (GGA) functional while setting the convergence limit of energy to 10^{-8} eV. SOC was included in all calculations in a self-consistent manner.

In several publications [15,17,18] the appearance of the second transition has been reported as a jump in magnetization M following a protocol in which the sample is cooled down to the lowest temperatures in a magnetic field ($B \parallel c$) large enough to ensure the magnetization is completely saturated, after which $M(T)$ has been measured while warming in a nominally zero field [field cooled/zero field warming (FC/ZFW)]. In Fig. 1(a) we present our results following the same protocol for three different samples, with three markedly different temperatures at which the jump occurs. The observed variation can be associated with shapes of the prepared samples (sketched alongside the respective curves) and their demagnetization factors N [25,26]. During a ZFW protocol, although $B_{\text{ext}} = 0$, a fully saturated sample experiences a demagnetization field $H_d = -NM$ whose effect is to cause a reversal at a lower temperature when N is larger. In the same way one can shift the reversal to lower or higher temperatures if $B_{\text{ext}} < 0$ or $B_{\text{ext}} > 0$, respectively [20]. Therefore, the jumps in magnetization $M \parallel c$ during the FC/ZFW protocols cannot be taken as evidence of a thermodynamic transition occurring around 125 K while their observation in that range of temperatures is a simple consequence of a specific sample geometry, typical for thin samples of $Co_3Sn_2S_2$. Additional evidence can be found in Figs. 1(b)–1(e) where hysteresis loops are presented for $S1$ and $S3$ samples in the range of temperatures spanning the purported transition. In Ref. [17] it has been suggested that one of the characteristic features is the change from the square-shaped loop into a more elongated one, with triangular wings. To the contrary, our results clearly show that neither $S1$ (large N) nor $S3$ (small N) change their behavior across 125 K. $S1$ exhibits a square loop only below 115 K while $S3$ up to 155 K. The only qualitative change occurs between 130 and 135 K where the reversal field for $S1$ goes from negative to positive, which agrees with the observed reversal temperature in the ZFW protocol of 132 K. Together with a lack of any feature seen in the ac response within the same temperature range (see below), we argue that there is no thermodynamic transition associated with $B \parallel c$ below T_C.

On the other hand, evidence presented by Kassem *et al.* [16] and especially recent reports [17,27] for $B \perp c$

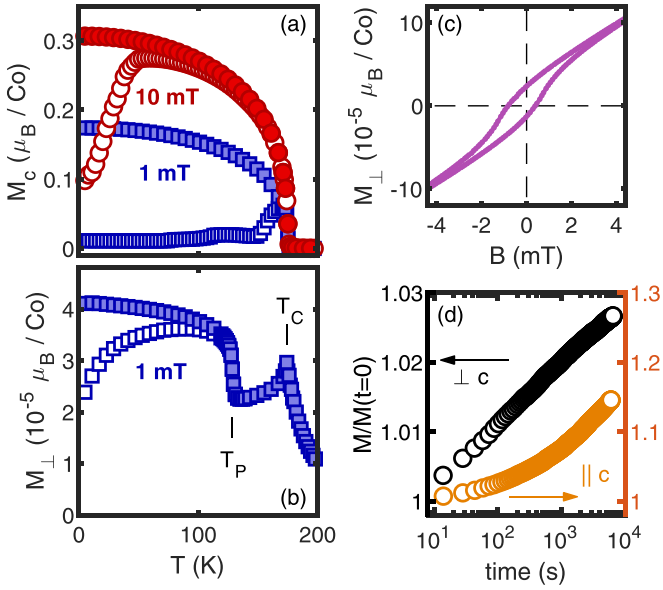

FIG. 2. (a) ZFC/FC protocols with $B \parallel c$ on $S3$. (b) ZFC/FC protocol with $B \perp c$ in 1 mT on $S1$. (c) The hysteresis loop at $T = 15$ K ($B \perp c$). (d) Time dependence of magnetization after ZFC to 50 K and $B = 1$ mT for two directions.

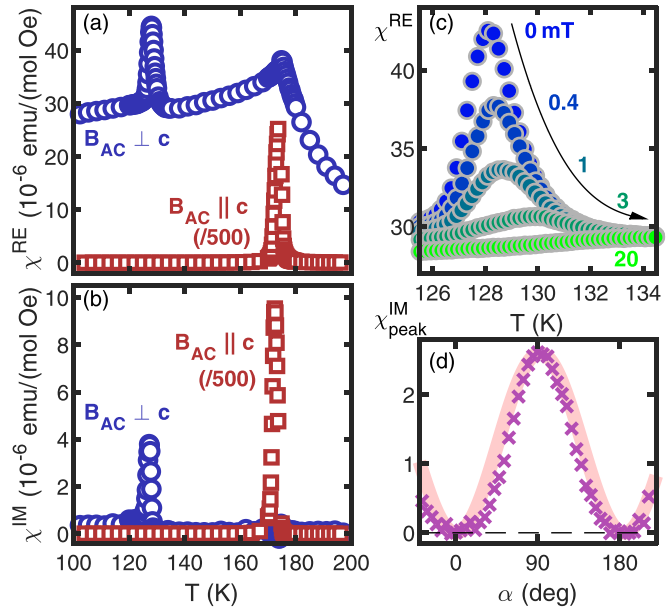

FIG. 3. (a) Real and (b) imaginary component of ac susceptibility ($B_{ac} = 1$ Oe) in $B = 0$ measured with 9.1 Hz on $S2$. (c) B dependence of χ^{RE} around T_P measured with 911 Hz. The amplitude of the peak decreases with increasing B, as indicated by the arrow. (d) The angular dependence of the peak in χ^{IM} at T_P measured with 911 Hz (crosses). The solid line indicates the $\sin^2\alpha$ dependence (see text).

unequivocally point to an intrinsic feature related to the magnetism of $Co_3Sn_2S_2$. In order to directly compare contributions to magnetization along different crystallographic directions we plot in Fig. 2 the $M(T)$ for $B \parallel c$ and $B \perp c$ following standard zero-field-cooled (ZFC)/field-cooled (FC) protocols. The main transition at T_C causes a sharp increase in M_c, followed by a ZFC/FC splitting stemming from the appearance of domains and pinning of domain walls. At the same time a clear maximum is observed in $M_\perp$ at T_C. On the other hand, a clear indication of a second transition is seen only in $M_\perp$. In a similar fashion as M_c increases and splits into separate ZFC and FC branches at T_C, $M_\perp$ follows the same behavior below $T_P = 128$ K, with values approximately four orders of magnitude smaller than M_c. The associated hysteresis loop, presented in Fig. 2(c), reveals that the splitting collapses already at 2 mT, significantly lower than for $B \parallel c$. An unequivocal decoupling of two directions can also be seen following a ZFC protocol to $T < T_P$ and observing a time dependence of magnetization after the magnetic field is turned on. Figure 2(d) reveals that the in-plane magnetization process cannot be seen as a simple projection of a (much larger) signal in M_c but it reflects a separate physical mechanism.

In Figs. 3(a) and 3(b) we demonstrate the overall behavior of ac susceptibility, the real χ^{RE} and the imaginary component χ^{IM}, for two directions in zero dc magnetic field. For $B_{ac} \parallel c$ both χ^{RE} and χ^{IM} show a sharp peak at T_C but no visible trace of the second transition. With $B_{ac} \perp c$, χ^{RE} shows a maximum at T_C, similar in shape to $M_\perp$, without any sizable feature in χ^{IM}. At T_P both components reveal a sharp, narrow peak, below which χ^{RE} continues a slow decrease while χ^{IM} remains near zero. Again the scale of response is orders of magnitude smaller for $B_{ac} \perp c$ but the features all remain well defined. There is a very weak frequency dependence of the maximum at T_P, similar in magnitude to the previous report [17].

One of the factors that strongly impacts the magnitude of the response at T_P is the dc magnetic field. As seen in Fig. 3(c), the peak is more than halved at 1 mT, while practically completely vanishes at 20 mT. One should note that a superconducting magnet, after being ramped down to a nominal zero field, still contains stray fields from pinned vortices, which can reach several mT (and cause a negative signal in nominally ZFC measurement conditions [5,16]). Combined with a typical sample mass of a couple of milligrams, it is easy to understand why in most cases the transition is hard to observe.

In order to reveal the angular dependence of the magnetic response around T_P, we turn to χ^{IM}. As displayed in Fig. 3(d), the amplitude of the peak closely follows a $\sim \sin^2\alpha$ dependence, where α is the angle between the ac magnetic field and the c axis. Such a type of a behavior is typical for projection-based vectors: One $\sin\alpha$ comes from the projection of the magnetic field onto a given axis, and the second one comes from the projection of magnetic moments back to the axis of the magnetic field. This indicates that the dissipation induced around T_P, and thus the order developing below T_P revealed by $M_\perp$ in Fig. 2(b), comes from the component of magnetic moments strictly perpendicular to the c axis. Note that χ^{IM} completely vanishes for $\alpha = 0$, unlike χ^{RE} which remains nonzero in the whole temperature range below T_C [Fig. 3(a)]. The lack of imaginary component is direct evidence against the idea of a thermodynamic transition occurring at T_P since crossing from the low-temperature phase into a ferromagnetic phase above T_P would involve a reconfiguration of moments and a substantial, more isotropic χ^{IM}.

Such a strictly in-plane component is incompatible with any known spin-glass scenario, which has been suggested solely based on a weak frequency dependence at T_P. It remains unclear how a spin-glass state would emerge from an FM state with a strong spin anisotropy or where is disorder, a necessary part of a glassy state, coming from. On the other hand, the weak in-plane dynamics can arise if the dominantly c-axis oriented magnetic moments are canted by a small angle. The question of canting of the moments in $Co_3Sn_2S_2$ has been addressed in several publications. Xu *et al.* [12] were first to use DFT calculations to calculate the total energy versus the canting angle, suggesting $M \parallel c$. Ghimire *et al.* [11] studied the magnetic-field-induced canting and its effect on the position and the total number of Weyl nodes. This was followed up by the μSR study [14] which suggested a sizable in-plane component forming a separate AFM phase, coexisting with the main (FM) one. Finally, recent DFT calculations by Solovyev *et al.* [28] addressed the stability of the FM order and again concluded that the lowest-energy configuration corresponds to moments being strictly parallel to the c axis. Contrary to those results is the more general, symmetry-based discussion about complex noncollinear structures in itinerant magnets with non-negligible SOC [29], which helped explain the emergence of canting in several systems, including Mn_3Sn and U_3P_4. The main conclusion is that the ferromagnetic structure with $M \parallel c$ is not symmetry protected, allowing for SOC-induced, small-angle canting of moments.

Motivated by these considerations, we performed self-consistent noncollinear magnetic calculations with VASP. We find that the magnetic moments in the resulting ferromagnetic ground state deviate from the c axis by a rather small angle $\theta_0 \approx 1.5^\circ$ forming the "umbrella structure" sketched in Fig. 4(a). The magnetic moment vectors obtained from the self-consistent calculations for the three Co sites are $(-0.008, -0.004, 0.345)$, $(0.008, -0.004, 0.345)$, and (0,0.009,0.345) in Bohr magneton units. We find that the in-plane components of the moments are quite small, but very robust to the changes in k-space mesh and initial electron density guess. Additionally, we calculated the total energy of the system with respect to the canting angle θ (focusing especially on the small-angle region), by constraining the direction of the moments at the three Co sites while allowing the size of the moments to evolve self-consistently. As shown in Fig. 4(b), the results of these calculations confirm that the deviation of moments from the c axis by an angle of $\theta_0 \approx 1.5^\circ$, yields a lower total energy per Co ion. It should be remarked that both previous reports [12,28] considered a relatively sparse grid, with steps in the range 5°–10°. Additionally, Solovyev *et al.* [28] performed the calculations without SOC, therefore our results represent a detailed numerical investigation of the full SOC-driven magnetic structure in $Co_3Sn_2S_2$. Note that the umbrella structure is fully compatible with a single Γ_2^+ irreducible representation [15].

We can return now to the question of the second transition at T_P and the development of the FM-like behavior of $M_\perp$ below T_P. It is evident that the FM component cannot arise from the umbrella structure as presented in Fig. 4(a), since the spin projections onto the kagome plane are forming a 120° structure, which is a fully compensated AFM arrangement. Instead, we propose a further modification which involves

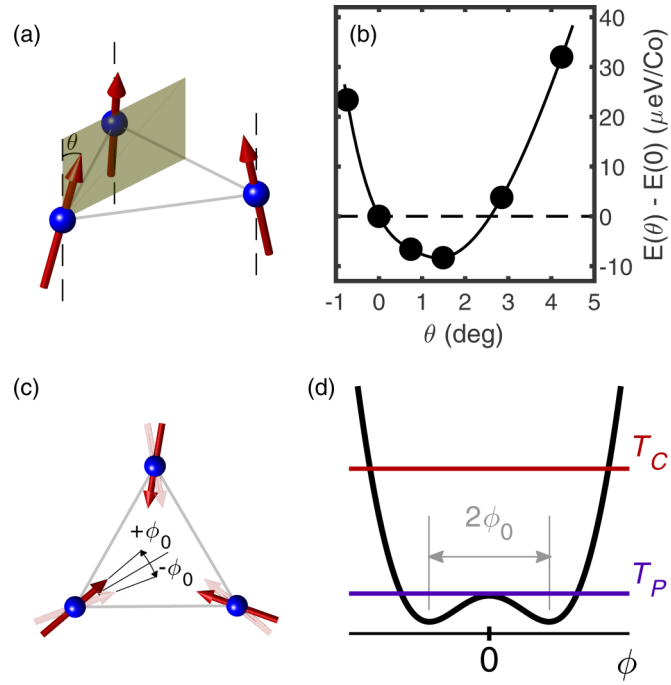

FIG. 4. (a) Sketch of the umbrella structure for $\theta > 0^\circ$. The moments rotate in the plane passing through the center of the triangle (dark yellow). (b) Total energy per cobalt ion for different angles relative to the energy at $\theta = 0^\circ$, as calculated by constrained DFT calculations. (c) The top view of the triangle with in-plane projections having two possible orientations given by $+\phi_0$ and $-\phi_0$. (d) The sketch of the energy potential with respect to the angle ϕ. Due to the small size of ϕ_0, the energy barrier between two orientations traps the moments only at $T = T_P < T_C$.

the rotation of moments around the c axis by an angle ϕ_0 [Fig. 4(c)]. Given that the transition at T_C is described within Γ_2^+ [15], such a rotation is forbidden by symmetry. However, once the temperature is lowered below T_C and the ordered state has been established, there are no symmetry-related constraints imposed on this type of a rotation. A simple model, presented in Fig. 4(d), encapsulates both of these aspects. It consists of a double-well potential with a barrier height significantly lower than T_C. Because the potential is symmetric in ϕ, the fluctuations of the order parameter within the critical region around T_C are still described by Γ_2^+ since $\langle\phi\rangle = 0$. Once the temperature is lowered to T_P, the ϕ rotations start to randomly freeze into $+\phi_0$ and $-\phi_0$, giving rise to the peak in ac susceptibility and its weak frequency dependence. A very small magnetic field can switch and eventually completely polarize those projections, ultimately giving rise to the dynamic completely different from the one observed for domain walls for $B \parallel c$. Alternatively, the double-well potential could arise *at* T_P, implying an additional energy scale for which there is no immediate evidence.

The value of ϕ_0 can be estimated from the in-plane FM component which is given by $M_\perp \sim M_c \sin\theta_0 \sin\phi_0$. Taking that $M_\perp/M_c \sim 10^{-4}$ and $\theta_0 \approx 1.5^\circ$, the amount of rotation perpendicular to the c axis is $\phi_0 \sim 0.2^\circ$–0.3°. Such a small value of ϕ_0 agrees with the model's assumption of a very small energy barrier while on the other hand represents a significant challenge for DFT and can even arise from contributions not

considered in our calculations. It also explains the lack of any feature in specific heat, since the entropy change across T_P would be negligibly small compared to phonon and magnon contributions.

Our findings are based on the careful control of all experimental parameters using large, high-quality single crystals. As such, they pose severe limits to hypotheses about the coexistence of secondary phases [14,17]. Note that those two proposals are mutually contradictory: The in-plane AFM phase has been suggested to occur above ∼90 K [14], reaching almost 70% volume fraction close to $T = T_C$ and having a different ordering temperature $T_{AFM} < T_C$. On the other hand, the spin-glass phase has been hypothesized to exist below $T = T_P$. No indication of T_{AFM} could be found below T_C, and neither was there any evidence of the dynamics of the phase boundary between the FM and AFM volume fractions. We confirmed the weak frequency dependence at T_P but for a true spin-glass phase the response would be expected to be more isotropic. We emphasize that many observations presented in those studies could find a natural explanation in a peculiar behavior of domain walls [7,18].

In summary, our results resolve several outstanding issues in $Co_3Sn_2S_2$. The second transition occurs at $T_P = 128$ K and is related to the freezing of a small component of magnetic moments perpendicular to the c axis. The jumps observed in magnetization parallel to the c axis are revealed to be sample dependent through the effect of demagnetization. Our SOC-based DFT calculations found that the moments are slightly canted away from the c axis, forming the umbrella configuration. The additional canting along the ϕ angle is needed to account for the in-plane component, whose origin at the moment remains unknown.

All the data files needed to plot figures presented in the paper can be found in [30].

I.Ž. acknowledges fruitful discussions with V. Ivanov, S. Savrasov, S. Acharya, and M. I. Katsnelson. J.-R.S. acknowledges support from the Singapore National Science Scholarship, Agency for Science Technology and Research. I.Ž. and J.-R.S. acknowledge support from the ERC Synergy grant HERO (Grant ID 810451). C.Y. and Y.S. were supported by the National Natural Science Foundation of China (No. 12004416 and No. U2032204) and the Informatization Plan of the Chinese Academy of Sciences (CAS-WX2021SF-0102). R.Y. was supported by the Swiss National Science Foundation (SNSF) Sinergia network "NanoSkyrmionics" (Grant No. CRSII5-171003). H.M.R. acknowledges the support from SNSF Projects No. 200020-188648 and No. 206021-189644. First-principles calculations were performed at the Swiss National Supercomputing Centre (CSCS) under Project No. s1008.

[1] B. Yan and S. C. Zhang, Rep. Prog. Phys. **75**, 096501 (2012).
[2] N. P. Armitage, E. J. Mele, and A. Vishwanath, Rev. Mod. Phys. **90**, 015001 (2018).
[3] L. Savary and L. Balents, Rep. Prog. Phys. **80**, 016502 (2017).
[4] N. Nagaosa, J. Sinova, S. Onoda, A. H. MacDonald, and N. P. Ong, Rev. Mod. Phys. **82**, 1539 (2010).
[5] E. Liu, Y. Sun, N. Kumar, L. Muechler, A. Sun, L. Jiao, S.-Y. Yang, D. Liu, A. Liang, Q. Xu, J. Kroder, V. Süß, H. Borrmann, C. Shekhar, Z. Wang, C. Xi, W. Wang, W. Schnelle, S. Wirth, Y. Chen *et al.*, Nat. Phys. **14**, 1125 (2018).
[6] D. F. Liu, A. J. Liang, E. K. Liu, Q. N. Xu, Y. W. Li, C. Chen, D. Pei, W. J. Shi, S. K. Mo, P. Dudin, T. Kim, C. Cacho, G. Li, Y. Sun, L. X. Yang, Z. K. Liu, S. S. P. Parkin, C. Felser, and Y. L. Chen, Science **365**, 1282 (2019).
[7] W. Schnelle, A. Leithe-Jasper, H. Rosner, F. M. Schappacher, R. Pöttgen, F. Pielnhofer, and R. Weihrich, Phys. Rev. B **88**, 144404 (2013).
[8] N. Morali, R. Batabyal, P. K. Nag, E. Liu, X. Xu, Y. Sun, B. Yan, C. Felser, N. Avraham, and H. Beidenkopf, Science **365**, 1286 (2019).
[9] Y. Okamura, S. Minami, Y. Kato, Y. Fujishiro, Y. Kaneko, J. Ikeda, J. Muramoto, R. Kaneko, K. Ueda, V. Kocsis, N. Kanazawa, Y. Taguchi, T. Koretsune, K. Fujiwara, A. Tsukazaki, R. Arita, Y. Tokura, and Y. Takahashi, Nat. Commun. **11**, 4619 (2020).
[10] Q. Wang, Y. Xu, R. Lou, Z. Liu, M. Li, Y. Huang, D. Shen, H. Weng, S. Wang, and H. Lei, Nat. Commun. **9**, 3681 (2018).
[11] M. P. Ghimire, J. I. Facio, J.-S. You, L. Ye, J. G. Checkelsky, S. Fang, E. Kaxiras, M. Richter, and J. van den Brink, Phys. Rev. Res. **1**, 032044(R) (2019).
[12] Q. Xu, E. Liu, W. Shi, L. Muechler, J. Gayles, C. Felser, and Y. Sun, Phys. Rev. B **97**, 235416 (2018).
[13] J. Shen, Q. Zeng, S. Zhang, W. Tong, L. Ling, C. Xi, Z. Wang, E. Liu, W. Wang, G. Wu, and B. Shen, Appl. Phys. Lett. **115**, 212403 (2019).
[14] Z. Guguchia, J. A. T. Verezhak, D. J. Gawryluk, S. S. Tsirkin, J.-X. Yin, I. Belopolski, H. Zhou, G. Simutis, S.-S. Zhang, T. A. Cochran, G. Chang, E. Pomjakushina, L. Keller, Z. Skrzeczkowska, Q. Wang, H. C. Lei, R. Khasanov, A. Amato, S. Jia, T. Neupert *et al.*, Nat. Commun. **11**, 559 (2020).
[15] J.-R. Soh, C. J. Yi, I. Zivkovic, N. Qureshi, A. Stunault, B. Ouladdiaf, J. A. Rodríguez-Velamazán, Y. G. Shi, H. M. Rønnow, and A. T. Boothroyd, Phys. Rev. B **105**, 094435 (2022).
[16] M. A. Kassem, Y. Tabata, T. Waki, and H. Nakamura, Phys. Rev. B **96**, 014429 (2017).
[17] E. Lachman, R. A. Murphy, N. Maksimovic, R. Kealhofer, S. Haley, R. D. McDonald, J. R. Long, and J. G. Analytis, Nat. Commun. **11**, 560 (2020).
[18] C. Lee, P. Vir, K. Manna, C. Shekhar, J. E. Moore, M. A. Kastner, C. Felser, and J. Orenstein, Nat. Commun. **13**, 3000 (2022).
[19] Y. Xu, J. Zhao, C. Yi, Q. Wang, Q. Yin, Y. Wang, X. Hu, L. Wang, E. Liu, G. Xu, L. Lu, A. A. Soluyanov, H. Lei, Y. Shi, J. Luo, and Z.-G. Chen, Nat. Commun. **11**, 3985 (2020).
[20] See Supplemental Material at http://link.aps.org/supplemental/10.1103/PhysRevB.106.L180403 for additional measurements of resistivity, Curie-Weiss behavior, magnetization switching vs magnetic field, sample dependence of in-plane magnetization,

frequency dependence of magnetic susceptibility and angular dependence around the main transition.
[21] G. Kresse and J. Furthmüller, Phys. Rev. B **54**, 11169 (1996).
[22] G. Kresse and J. Hafner, Phys. Rev. B **47**, 558 (1993).
[23] P. Vaqueiro and G. G. Sobany, Solid State Sci. **11**, 513 (2009).
[24] J. P. Perdew, K. Burke, and M. Ernzerhof, Phys. Rev. Lett. **77**, 3865 (1996).
[25] D.-X. Chen, J. Brug, and R. Goldfarb, IEEE Trans. Magn. **27**, 3601 (1991).
[26] D.-X. Chen, E. Pardo, and A. Sanchez, IEEE Trans. Magn. **38**, 1742 (2002).
[27] Q. Zhang, S. Okamoto, G. D. Samolyuk, M. B. Stone, A. I. Kolesnikov, R. Xue, J. Yan, M. A. McGuire, D. Mandrus, and D. A. Tennant, Phys. Rev. Lett. **127**, 117201 (2021).
[28] I. V. Solovyev, S. A. Nikolaev, A. V. Ushakov, V. Y. Irkhin, A. Tanaka, and S. V. Streltsov, Phys. Rev. B **105**, 014415 (2022).
[29] L. Sandratskii, Adv. Phys. **47**, 91 (1998).
[30] https://doi.org/10.5281/zenodo.7316664.